Applied Physics Letters ARTICLE scitation.org/journal/apl

Microwave annealing of silicon solar cells

Cite as: Appl. Phys. Lett. **122**, 142101 (2023); doi: 10.1063/5.0127896
Submitted: 25 September 2022 · Accepted: 21 March 2023 ·
Published Online: 3 April 2023

Binesh Puthen Veettil,[1,a)] Yuchao Zhang,[2] David Payne,[1] Mattias Juhl,[1] Shujuan Huang,[1] Brett Hallam,[2] and Darren Bagnall[1]

AFFILIATIONS

[1]School of Engineering, Macquarie University, Macquarie Park NSW 2109, Australia
[2]School of Photovoltaic and Renewable Energy Engineering, University of New South Wales, Sydney NSW 2207, Australia

[a)]**Author to whom correspondence should be addressed:** binesh.puthenveettil@mq.edu.au

ABSTRACT

The microwave annealing of semiconductor devices has not been extensively researched and is rarely utilized in industry, yet it has the potential to significantly reduce the time and cost associated with large-volume semiconductor processing, such as the various heating and annealing processes required in the manufacture of photovoltaic modules. In this paper, we describe microwave annealing of silicon solar cells, the effective passivation of light-induced defects, and a reduction in light-induced degradation. We find that silicon solar cells are heated rapidly in a microwave field and that effective B–O defect passivation can be achieved by microwave processing in less than 2 s. Microwave annealing yields similar results as compared to rapid thermal annealing.

Microwave heating is used in many manufacturing industries for its energy efficiency and economic viability in the provision of fast, simple, and cost-effective processes.[1–4] Microwave heating is direct, volumetric, and selective. Under oscillating electric and magnetic fields of microwave radiation, heat generation results from energy losses in the material–radiation interaction, and these energy losses typically include "conduction losses" in metals or "dipole polarization losses" in dielectrics.[5,6] In many instances, the electromagnetic interactions of semiconductors lie somewhere in-between or significantly not different to those of metals and dielectrics, and in the absence of published data, it is reasonable to assume that microwaves can interact with conventional semiconductors, such as silicon, and thereby affect heating or annealing processes. Microwave heating in semiconductors is likely to depend on many material and structural parameters and characteristics but likely to be critically dependent upon variables such as the density of free-carriers and the lattice temperature.

Intrinsic crystalline silicon, in its purest form, is a poor absorber of microwaves;[7] however, Sameshima *et al.*[8] have shown that the optical excitation of free-carriers can modulate microwave transmission through silicon with close to complete transparency and close to complete opacity depending on the wafer thickness and the optical excitation density (or effective resistivity).[8] Although Sameshima *et al.* did not determine the extent to which microwaves were reflected or absorbed, we can infer that both reflection and absorption are responsible for the reduction in transmission and that the absorption is likely to generate heat through conduction losses.

Although available for more than seven decades, microwave heating is relatively new to semiconductor processing. The first instances of susceptor-assisted microwave annealing (MWA) were used for processing ultra-shallow semiconductor PN junctions in 1997,[9] microwave RF plasmas are also commonly used in plasma enhanced chemical vapor deposition (PECVD) of semiconductors dating back to the 1950s,[10] and susceptor-assisted microwave annealing has been used to create shallow junctions on As^+ ion-implanted silicon wafers.[7] Microwave annealing techniques have been used in silicon photovoltaics to induce crystallization through susceptor-assisted microwave heating,[11,12] but there has been very little published in direct microwave annealing until a very recent report on the microwave activation of phosphorus dopants in silicon nanosheets.[13]

The silicon photovoltaics industry is currently the biggest consumer of electronic grade silicon, with the projected growth to 4500 GW by 2050.[14] Some energy-intensive steps in solar cell manufacturing, specifically co-firing and hydrogenation, are essential for mitigating light-induced degradation (LID) that can reduce cell efficiency by up to 10%.[15] Dark annealing (DA) has shown to reverse the adverse effects of LID on solar cell performance, although the results are temporary. LID is dominated by light-induced formation of deep traps associated with boron–oxygen (B–O) complexes.[16,17] The effectiveness of dark annealing and hydrogenation in mitigating B–O defects has been published elsewhere.[18,19] These annealing processes are usually performed using traditional thermal or optical techniques

and are found to deactivate recombination centers resulting in increased performance.[20]

This work is motivated by the desire to see if microwave annealing can be used to mitigate LID in silicon solar cells and thereby help to reduce the cost of solar energy. In this work, we investigate the annealing of cz-silicon solar cells and compare the defect passivation with conventional but energy-intensive processing steps of dark annealing and the advanced hydrogenation process (AHP).[17,21] We further investigate the effectiveness of combining dark co-firing and hydrogenation steps with a view to achieving a shorter combined process time.

Passivated emitter rear contact (PERC) silicon solar cell precursors,[22] fabricated on boron-doped silicon wafers with a thickness of 180 μm and with resistivities in the range of 0.5 to 1 Ω cm, were used for these experiments. These wafers received alkaline etching for the purpose of surface texturing, followed by acidic cleaning to remove metallic impurities on the wafer surface. Following the chemical clean, $POCl_3$ diffusion was performed, resulting in an n^+ emitter with a sheet resistivity of $\sim$100 $\Omega/\square$ on each side. Subsequently, the phosphor silicate glass (PSG) layer on the front side and n^+ diffused regions at the edge and rear side were removed via chemical etching. SiN_x:H layers with a thickness of around 80 nm and a refractive index of 2.07 at 633 nm were deposited using a plasma-enhanced chemical vapor deposition tool (Centrotherm) on the front side. Al_2O_3 layers with a thickness of $\sim$7 nm were deposited using atomic layer deposition on the rear side capped with another 140 nm thick SiN_x layer.

The cells were laser cleaved into 4×4 cm^2 samples. The samples were then subjected to various processing stages, including firing, dark annealing (DA), advanced hydrogenation process (AHP), and microwave annealing (MWA).[17,23] The samples were divided into three groups, namely, MWA, AHP, and MWA + AHP. Some samples were rapid thermal annealed (RTA) instead of MWA. Control group samples did not go through MWA but all other process steps. The various processing stages of the different sample groups are shown in Table I.

The AHP step was performed on a hotplate under illumination with a 938 nm, 0.5 ms pulse fiber coupled laser operating at 2 kHz. The average irradiance was estimated to be 70.5 kW/m^2. The hotplate was kept at 250 °C. Further details of this experiment have been published previously.[17] The AHP step was performed for 8 s. The light soaking (LS) step was performed for 48 h under a halogen lamp illumination at an intensity of 0.78 kW/m^2 at 40 °C.[17]

Selected samples were processed using a custom-made, computer-controlled, 1000 W multi-mode microwave cavity operating at 2.45 GHz frequency. This equipment is a modified version of the laboratory microwave BP125 from Microwave Research and Applications, Inc. The microwave cavity is of dimensions $330 \times 330 \times 204.7$ mm^3 and the samples were placed 60 mm from the bottom wall of the cavity where the heating was found to be maximum.

TABLE I. Details of the processing steps. The zero-seconds microwave-processed samples from group 1 are used as controls.

	Group 1	Group 2	Group 3
780 °C Firing	✓	✓	✓
Dark annealing 250 °C 10 min	✓	✓	✓
LED light soaking 48 h	✓	✓	✓
Advanced hydrogenation	···	✓	✓
Microwave processing/ rapid thermal annealing	0, 2, 4, 8, and 16 s	···	2, 4, 8, and 16 s
LED light soaking 48 h	✓	✓	✓

Muffle boxes made of alumina–silica composite were used for holding the samples and protecting the magnetron from the generated heat from the samples. Silicon carbide (SiC) susceptor blocks were used as dummy loads to absorb excessive radiation that builds up inside the cavity. The samples were heated directly using microwaves (and not by the indirect heat from the SiC susceptors). The samples were irradiated in the microwave cavity for 1, 2, 4, 8, and 16 s. The temperature was monitored using an infrared thermometer (OS-MINIUSB-SN201) placed through a 1-in. diameter microwave-proof hole in the cavity. The infrared thermometer was calibrated using a fiber optic thermometer (OMEGA FOM-H201) and accurate to be within 10 °C.

The samples were characterized after each processing step. The effective lifetime was measured using a photoconductance lifetime tester (WCT-120, Sinton Instruments) with nine points sampled per wafer[24] after each processing step. The lifetime data were corrected for Auger recombination.[25] The effective lifetime, thus, extracted at the injection level of 1×10^{15} cm^{-3} ($\sim$10% of the base dopant concentration) indicates the impact of various defects, including, B–O, bulk, and surface defects.[26] Calibrated implied voltage maps were obtained from photoluminescence (PL) images using a BT-Imaging LIS-R3 tool.[27]

Intrinsic silicon is not a good absorber of microwaves,[8] however, in the case of solar cells, the highly doped n-type diffusion regions and the lightly doped, p-type bulk regions provide enough charge carriers[28] to contribute to microwave absorption and heating. We have observed our samples to heat up rapidly as a result of microwave absorption. Figure 1 shows the heating profile of a silicon sample in the microwave cavity operated at full power (1000 W). The sample heated up to $\sim$500 °C within 2 s of applying the microwave power and then was found to reach a thermal equilibrium due to natural thermal exchange with the surroundings. The fluctuations seen in Fig. 1 are caused by the heavy electromagnetic interference on the temperature signal. Around 148 W of microwave power was calculated to be absorbed by the silicon sample (see the supplementary material) and the rest was absorbed by the dummy loads. This result shows that volumetric heating rates as high as 250 °C/s are possible for silicon wafers used in photovoltaics.

The amount of microwave power absorbed by a material will depend on its complex permittivity (ε^*) modified by the conduction term,[29]

$$\varepsilon^* = \varepsilon' - i\varepsilon'' - \left(\frac{i\sigma}{\omega\varepsilon_0}\right), \quad (1)$$

where ε' and ε'' are the real and imaginary parts of the dielectric constant, σ is the conductivity, ω is the angular frequency of the radiation, and ε_0 is the dielectric constant of free space. The conductivity term can be affected externally by doping or excitation.[28] In this case, we believe that the heavily doped diffusion region provides the opportunity for the rapid heating of the sample and is attributed to the conduction loss term in the equation.

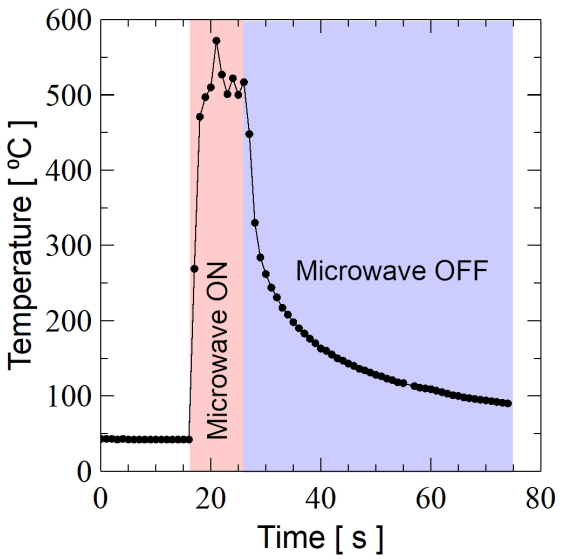

FIG. 1. Heating profile of cz-silicon solar cell sample in the microwave cavity. The red shaded area shows the heating of the sample when the microwave was ON, and the blue shaded area shows the natural cooling when the microwave was OFF.

At the maximum electric field, the microwave power absorbed per unit volume within the skin depth region (P_{MW}) can be represented by the following formula:

$$P_{MW} = \frac{1}{2}\sigma E^2 \; Watts/m^3, \tag{2}$$

where E is the electric field strength (V/m) inside the cavity.

The effects of the MWA process on group 1 samples were characterized using PL imaging and carrier lifetime measurements. Figure 2 (left) shows the changes in the PL image intensity of the samples as they were subjected to various processing steps. The initial DA step was performed to ensure a reference starting point by eliminating the B–O defects already present in the sample. The samples after dark annealing showed high PL intensity with a corresponding effective lifetime of more than 60 μs. After introducing B–O defects by the first light soaking step, the PL intensity and the effective lifetime reduced by more than 20 μs. The PL intensity was restored after MWA process of the samples for 4 s. Figure 2 (right) shows the effective lifetime of the samples that were MWA processed for 1, 2, 4, 8, and 16 s. MWA seems to revive the effective lifetime with less than 2 s of microwave heating, and further improvements come with the longer processing times. The corresponding PL intensity of the sample annealed for 4 s shows very bright features and uniformity (Fig. 2, left). The second light soaking process did not reduce the lifetime of the samples lower than the initial light soaking process for all samples that were microwave processed for more than 2 s. The second light soaking step had a lower impact on the MWA samples as compared to the control and the 1-s MWA samples. The effective lifetime and the corresponding PL intensity retained some of their initial values after the second light soaking step, which can be seen as the brighter image for the light soaking sample in Fig. 2 on the left. Tests on group 1 samples reveal that the B–O degradation can be recovered by MWA, same as dark annealing at beyond 250 °C; however, similar to dark annealing, the defects reappear after subsequent exposure to light.[30]

Microwave heating of dielectric samples in cavities is known to have hot and cold spots. However, the microwave annealed results (post-MWA and post-second LS) below show that the heating in the samples was fairly uniform, with no bright or dark spots in the PL image. This is due to the higher thermal conductivity of silicon evening out the temperature differences in the $4 \times 4\,cm^2$ sample. The temperature at five different points on two group 1 samples is shown as Fig. S1 in the supplementary material. Figure 3 shows the repeatability of the microwave annealing experiments—five samples of a similar effective lifetime after the first LS were selected for the repeatability test. The effective lifetimes of these samples varied between 41 and 42.5 μs. These samples were heated (one at a time) in the microwave cavity at 1000 W power setting for 16 s. The samples were placed at the exact location in the cavity. The longer heating time was chosen to minimize errors in the start and stop timings. All samples showed improvements in the effective lifetime with a tight distribution between 77 and 74 μs—less than 4% deviation.

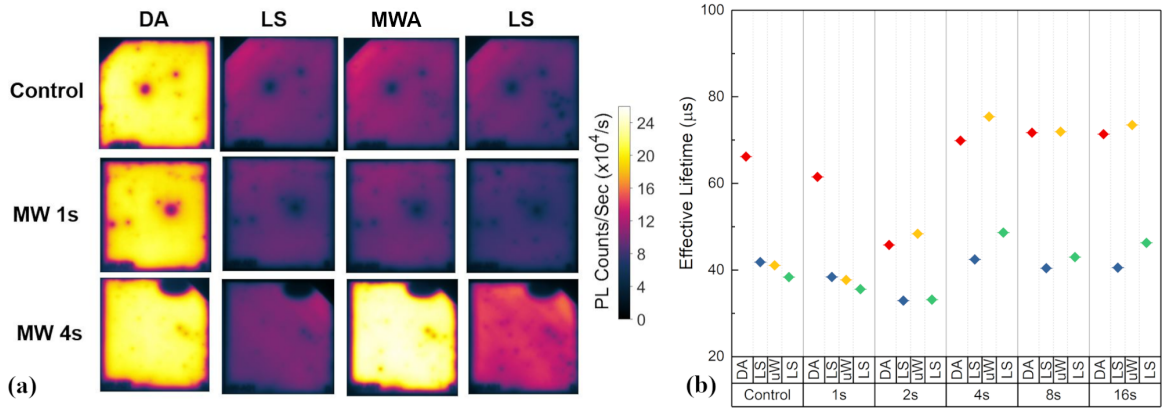

FIG. 2. PL images (left) and the effective lifetime (right) of group 1 samples after four processing steps—dark annealing (DA), light soaking (LS), microwave processing (MWA), and the second round of LS are shown for various MWA processing times. The control sample did not go through MWA but through all other processing steps.

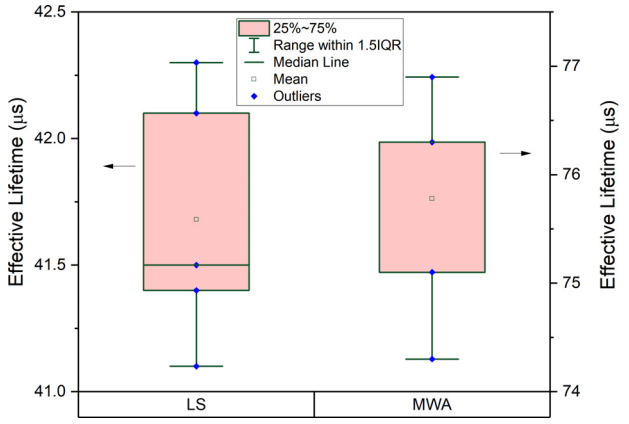

FIG. 3. The distribution of effective lifetimes of five samples from group 1 samples taken after the first light soaking (LS) and microwave annealing (MWA) for 16 s at 1000 W power setting.

Herguth *et al.* reported the permanent deactivation of the B–O defects by illuminated annealing.[31] One of these annealing approaches is advanced hydrogenation process (AHP).[21] AHP requires a high-power laser illumination source with high intensity (~40 KW/m^2). Here, we compared the effective lifetime of samples processed by MWA (non-illuminated) with those treated by AHP to understand the relative effectiveness of MWA in passivating the B–O defects. The 16 s MWA processed samples were used for comparison with AHP processed samples. AHP + MWA represents the process where samples were MWA processed after AHP.

Results from group 1, 2, and 3 samples are shown in Fig. 4. AHP, MWA, and AHP + MWA all show an increase in lifetime over the LS samples (Fig. 4, left). For comparison, we normalized the effective lifetime of the sample at each stage with the effective lifetime after the first LS. Table II shows the changes in the normalized effective lifetime in percentage. MWA was comparable to AHP in improving the carrier lifetime, showing an improvement of 87.5% compared to 90.5% by AHP. However, after the second round of the LS step, there was a significant decrease in lifetime percentage for the MWA processed samples. This was true for AHP + MWA processed samples as well. Ideally, AHP treated samples should not degrade during light soaking. The decrease in lifetime after the second LS step is likely caused by a non-optimized AHP process. The actual lifetime curves (Fig. 4, right) indicate that the changes in lifetime came from SRH defects. The comparison of the lifetimes after the first and second LS steps shows that only AHP could retain the defect reduction (or passivation). The lower lifetime in the AHP + MWA samples might be because of the rapid release of hydrogen from passivated recombination centers of B–O defects. Finely tuned MWA processing time and/or power may be needed to prevent the excessive loss of hydrogen. Results in Fig. 4 and Table I show that although MWA is effective in passivating B–O defects, the effects are not permanent. MWA may be thought of as an alternative way to do RTA.

TABLE II. Effective lifetime in percentage after each processing stage compared to the lifetime after the first light-soaking step.

	Effective lifetime after the first LS (μs)	Percentage increase after MWA/AHP	Percentage decrease after the second LS
AHP	42	90.5	26
MWA	40	87.5	37
AHP + MWA	42.5	91	41

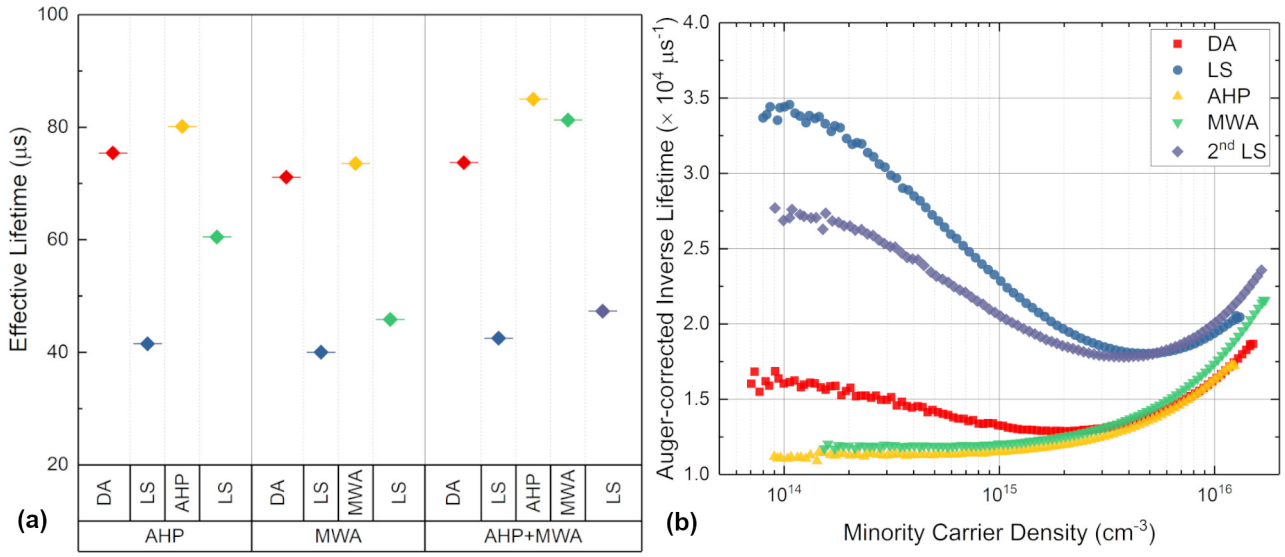

FIG. 4. (Left) The effective lifetimes of samples from groups 1, 2, and 3 at various processing stages. Lifetimes are shown for multiple processing stages—dark annealing (DA), light soaking (LS), advanced hydrogenation process (AHP), and microwave annealing (MWA). Here, MWA was applied for 16 s. Group 3 samples underwent AHP followed by MWA processing (AHP + MWA). (Right) The lifetime curves for samples from group 3.

To study the effectiveness of MWA as a rapid annealing technique, we compared the effective lifetime of MWA samples and RTA-processed samples. The RTA equipment used was a Jipelec JetFirst 200 system with infrared lamp heaters. The set thermal profile was matched to microwave processing thermal profiles (500 °C in 2 s). Figure 5 shows the effective lifetimes of samples from group 1 for 4, 8, and 16 s of processing time in RTA and MWA. The nonpermanent passivation of B–O defects was found in both sets of samples. It can be seen that during either RTA or MWA, the lifetime completely recovers from the LS defects, and the changes are relatively similar for each processing step. The recovery is the highest in 4 s-RTA/MWA processed samples. RTA and MWA processing parameters require further optimization to maximize the lifetime recovery.

In the context of microwave cavity experiments, the presence of metal contacts or fingers on cells can affect the field distribution and absorption within the cavity. Although the metallization fraction is typically small, with finger widths of approximately 40 μm, the impact cannot be ignored. Fortunately, the problems caused by metals can be minimized through proper alignment of the fingers with respect to the electric field and by using higher frequencies or higher harmonics. These measures further reduce the impact of the metal contacts on the field distribution and absorption, resulting in more accurate experimental results.

In this work, we investigated the microwave annealing of cz-silicon solar cells for defect passivation. We have found that rapid heating of the silicon at a rate of 250 °C/s is achievable and this heating is able to passivate light-induced defects in silicon cells with less than 2–4 s of microwave exposure. PL images and the effective lifetime data indicate a significant improvement in defect density in all samples. Microwave annealed samples are found to retain some defect passivation over the second round of light-induced degradation. The B–O defect passivation by microwave annealing was not as stable as compared to the passivation by the advanced hydrogenation process.

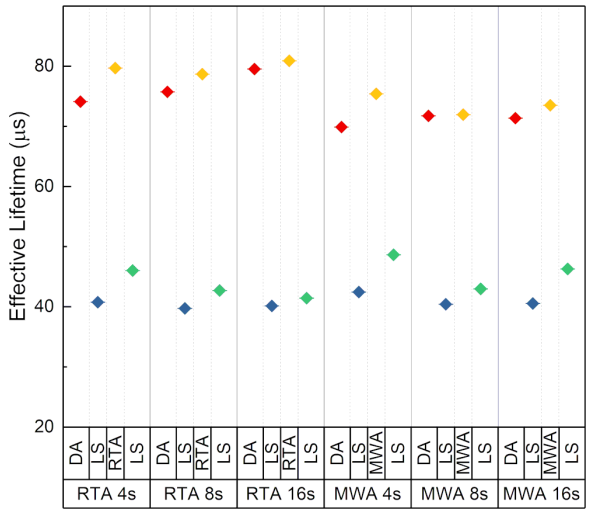

FIG. 5. Comparison between the effective lifetimes of MWA and RTA processed group 1 samples. Lifetimes are shown for multiple processing stages—dark annealing (DA), light soaking (LS), rapid thermal annealing (RTA), and microwave annealing (MWA).

Effective carrier lifetime comparison with the rapid thermal annealed samples shows that MWA is effective as a rapid thermal process. Although currently only of academic interest, these results open up an opportunity to use microwave annealing as an alternative rapid thermal process that can combine firing and advanced hydrogenation processes, significantly reducing both time and cost. We have shown that absorption of microwaves in a semiconductor can be used as an effective annealing method and this may provide many opportunities to reduce both cost and thermal load within the semiconductor industry. For now, however, the further work is required to fully understand the physical mechanisms and to determine the dielectric parameters for semiconductors across the microwave spectrum so that processes can be optimized.

See the supplementary material for the calculations that estimate the microwave power absorbed by the samples and the statitistcal data of temperature monitored at five points from two group 1 samples.

The authors acknowledge ACAP funding for enabling this work. This program has been supported by the Australian Government through the Australian Renewable Energy Agency (ARENA). Responsibility for the views, information, or advice expressed herein is not accepted by the Australian Government.

AUTHOR DECLARATIONS

Conflict of Interest

The authors have no conflicts to disclose.

Author Contributions

Binesh Puthen Veettil: Conceptualization (lead); Data curation (lead); Investigation (equal); Methodology (lead); Writing – original draft (lead). **Yuchao Zhang:** Data curation (equal); Investigation (supporting). **David Payne:** Funding acquisition (equal); Methodology (supporting); Writing – review & editing (equal). **Mattias Klaus Juhl:** Formal analysis (supporting); Writing – review & editing (equal). **Shujuan Huang:** Funding acquisition (equal); Resources (supporting); Writing – review & editing (equal). **Brett Jason Hallam:** Data curation (supporting); Formal analysis (equal); Funding acquisition (equal); Supervision (supporting); Writing – review & editing (equal). **Darren Bagnall:** Formal analysis (equal); Funding acquisition (equal); Methodology (equal); Writing – review & editing (equal).

DATA AVAILABILITY

The data that support the findings of this study are available from the corresponding author upon reasonable request.

REFERENCES

[1]R. J. Meredith, J. Elastomers Plast. **8**, 191 (1976).
[2]Z. Huang, M. Gotoh, and Y. Hirose, J. Mater. Process. Technol. **209**, 2446 (2009).
[3]J. Mullin, "Microwave processing," in *New Methods of Food Preservation*, edited by G. W. Gould (Springer US, Boston, MA, 1995), pp. 112–134.
[4]M. T. K. Kubo, É. S. Siguemoto, E. S. Funcia, P. E. D. Augusto, S. Curet, L. Boillereaux, S. K. Sastry, and J. A. W. Gut, Curr. Opin. Food Sci. **35**, 36 (2020).
[5]R. E. Hummel, *Electronic Properties of Materials* (Springer, New York, NY, USA, 2011).

[6]T. E. Seidel, D. J. Lischner, C. S. Pai, R. V. Knoell, D. M. Maher, and D. C. Jacobson, Nucl. Instrum. Methods Phys. Res. B **7–8**, 251 (1985).
[7]R. N. P. Vemuri, M. J. Gadre, N. D. Theodore, W. Chen, S. S. Lau, and T. L. Alford, J. Appl. Phys. **110**, 34907 (2011).
[8]T. Sameshima, H. Hayasaka, and T. Haba, Jpn. J. Appl. Phys., Part 1 **48**, 021204 (2009).
[9]H. Amada, U.S. patent US6051483A (4 June 1997).
[10]K. M. Poole, Proc. Phys. Soc. B **66**, 542 (1953).
[11]S. Kimura, K. Ota, M. Hasumi, A. Suzuki, M. Ushijima, and T. Sameshima, Appl. Phys. A **122**, 695 (2016).
[12]T. Gunawansa, Z. Zhao, N. D. Theodore, A. R. Lanz, and T. L. Alford, in *EPD Congress 2015*, edited by J. A. Yurko, A. Allanore, L. Bartlett, J. Lee, L. Zhang, G. Tranell, Y. Meteleva-Fischer, S. Ikhmayies, A. S. Budiman, P. Tripathy, and G. Fredrickson (Springer International Publishing, Cham, 2016), pp. 141–148.
[13]C. H. Tsai, C. P. Savant, M. J. Asadi, Y. M. Lin, I. Santos, Y. H. Hsu, J. Kowalski, L. Pelaz, W. Y. Woon, C. K. Lee, and J. C. M. Hwang, Appl. Phys. Lett. **121**, 052103 (2022).
[14]IRENA, "End-of-life management: Solar Photovoltaic Panels" (International Renewable Energy Agency, 2016).
[15]F. Kersten, P. Engelhart, H. Ploigt, A. Stekolnikov, T. Lindner, F. Stenzel, M. Bartzsch, A. Szpeth, K. Petter, J. Heitmann, and J. W. Müller, in *42nd Photovoltaic Specialists Conference* (IEEE, 2015), pp. 1–5.
[16]J. Schmidt, A. G. Aberle, and R. Hezel, in *Conference Record of the IEEE Photovoltaic Specialists Conference* (IEEE, 1997).
[17]B. J. Hallam, C. E. Chan, R. Chen, S. Wang, J. Ji, L. Mai, M. D. Abbott, D. N. R. Payne, M. Kim, D. Chen, C. Chong, and S. R. Wenham, Jpn. J. Appl. Phys., Part 1 **56**, 08MB13 (2017).
[18]K. Bothe and J. Schmidt, J. Appl. Phys. **99**, 13701 (2006).
[19]B. Sopori, J. Electron. Mater. **31**, 972 (2002).
[20]P. Karzel, J. Junge, and G. Hahn, in 24th European Photovoltaic Solar Energy Conference, Hamburg (2009).
[21]P. Hamer, S. Wang, B. Hallam, S. Wenham, C. M. Chong, A. Wenham, and M. Abbott, Phys. Status Solidi RRL **9**, 111 (2015).
[22]A. W. Blakers, A. Wang, A. M. Milne, J. Zhao, and M. A. Green, Appl. Phys. Lett. **55**, 1363 (1989).
[23]B. J. Hallam, P. G. Hamer, S. Wang, L. Song, N. Nampalli, M. D. Abbott, C. E. Chan, D. Lu, A. M. Wenham, L. Mai, N. Borojevic, A. Li, D. Chen, M. Y. Kim, A. Azmi, and S. Wenham, Energy Procedia **77**, 799 (2015).
[24]R. A. Sinton, A. Cuevas, and M. Stuckings, in *Conference Record of the Twenty Fifth IEEE Photovoltaic Specialists Conference* (IEEE, 1996).
[25]A. Richter, F. Werner, A. Cuevas, J. Schmidt, and S. W. Glunz, Energy Procedia **27**, 88 (2012).
[26]A. Cuevas and D. Macdonald, Sol. Energy **76**, 255 (2004).
[27]T. Trupke, R. A. Bardos, M. C. Schubert, and W. Warta, Appl. Phys. Lett. **89**, 044107 (2006).
[28]S. M. Sze, *Semiconductor Devices—Physics and Technology*, 2nd ed. (John Wiley and Sons Inc., 2002).
[29]J. D. J. D. Kraus, in *Electromagnetics*, edited by J. D. Kraus and K. R. Carver (McGraw-Hill, New York, 1973).
[30]J. Schmidt, A. G. Aberle, and R. Hezel, in *Conference Record of the Twenty Sixth IEEE Photovoltaic Specialists Conference* (IEEE, 1997), pp. 13–18.
[31]A. Herguth, G. Schubert, M. Kaes, and G. Hahn, in *IEEE 4th World Conference on Photovoltaic Energy Conference* (IEEE, 2006), pp. 940–943.